MEDICAL SCIENCE MONITOR

CLINICAL RESEARCH

e-ISSN 1643-3750
© Med Sci Monit, 2016; 22: 4186-4192
DOI: 10.12659/MSM.897255

Received: 2015.12.24
Accepted: 2016.02.23
Published: 2016.11.04

# Association Between microRNA-125a rs12976445 C>T Polymorphism and 18F-Fluorodeoxyglucose ($^{18}$FDG) Uptake: Clinical and Metabolic Response in Patients with Non-Small Cell Lung Cancer

Authors' Contribution:
Study Design A
Data Collection B
Statistical Analysis C
Data Interpretation D
Manuscript Preparation E
Literature Search F
Funds Collection G

ABCDE 1 Zhina Zang
BCDE 1 Wenhua Guan
BCD 2 Diansen Chen
BCD 2 Yan Han
DEF 2 Zhan Shi
CEF 2 Jinjin Zhou

1 Department of Nuclear Medicine, The Affiliated Hospital of Henan University of Science and Technology, Luoyang, Henan, P.R. China
2 Department of Medical Imaging, The Affiliated Hospital of Henan University of Science and Technology, Luoyang, Henan, P.R. China

**Corresponding Author:** Wenhua Guan, e-mail: petfdg@126.com
**Source of support:** Departmental sources

**Background:** MicroRNA-125a (miR-125a) has been involved with many diseases, such as hepatocellular carcinoma and inflammation. In this study, we aimed to investigate the molecular mechanism, including the potential regulator and signaling pathways, of vascular endothelial growth factor (VEGF).

**Material/Methods:** We divided the participants into 3 groups by rs12976445 genotype and performed chi-square tests to evaluate the differences between CC and CT+TT groups for sex, age, grading, pT category, metastases, and fludeoxyglucose F18 injection ($^{18}$FDG) metabolism.

**Results:** We found all variables to be statistically significant. We searched the miRNA database online (*www.mirdb.org*) with the "seed sequence" located within the 3-prime untranslated region (3' UTR) of the target gene and then validated VEGF to be the direct gene via luciferase reporter assay system. We also established the negative regulatory relationship between MiR-125a and VEGF by studying the relative luciferase activity. We conducted real-time polymerase chain reaction and Western blot analysis to study the mRNA and protein expression level of VEGF among different groups (CC=18, CT=8, TT=3) or cells treated with scramble control, miR-125a mimics, VEGF RNA, and MiR-125a inhibitors.

**Conclusions:** We validated the negative regulatory relationship between MiR-125a and VEGF and found that rs12976445 may function as a biomarker to predict metabolism of $^{18}$FDG.

**MeSH Keywords:** Basal Metabolism • Carcinoma, Non-Small-Cell Lung • MicroRNAs

**Full-text PDF:** http://www.medscimonit.com/abstract/index/idArt/897255

2748 1 4 27

This work is licensed under Creative Common Attribution-NonCommercial-NoDerivatives 4.0 International (CC BY-NC-ND 4.0)



Indexed in: [Current Contents/Clinical Medicine] [SCI Expanded] [ISI Alerting System] [ISI Journals Master List] [Index Medicus/MEDLINE] [EMBASE/Excerpta Medica] [Chemical Abstracts/CAS] [Index Copernicus]

## Background

18F-fluorodeoxyglucose ($^{18}$FDG), the glucose analog, which is combined with positron emission tomography (PET), has been developed as a critical clinical tool for monitoring of response, staging, and detection of cancers and is currently adopted in clinical management of numerous malignancies. Still, the mechanisms underlying uptake of $^{18}$FDG in cancer remain unclear, and the existing literature is contradictory and mixed. The German physician and chemist Otto Warburg revealed there was an increased glucose demand in Ehrlich ascites cancer cells. He noted that cancer cells tended to metabolize glucose by mitochondrial dysfunction-associated aerobic glycolysis even in the presence of ample oxygen, the so-called Warburg effect [1]. A consensus has been reached that increased glucose demand is a fundamental cancer feature, which has been exploited clinically to detect cancers by $^{18}$FDG PET.

The density and integrity of the vascular network contribute to the major determinant of $^{18}$FDG and glucose. A recent study revealed a positive correlation between microvessel density and $^{18}$FDG [2]. Vascular endothelial growth factor (VEGF), a dimeric glycoprotein that presents a high expression level in most malignancies, accounts for the most important inducer or regulator angiogenesis or vascular growth [3].

MicroRNAs (miRNAs) are evolutionarily conserved, single-stranded RNA molecules approximately 22 nucleotides in length that regulate expression of genes negatively by directing sequence-specific degradation or inhibiting translation of target messenger RNA (mRNA) [4,5]. MiRNA genes are predicted to account for 1% to 5% of the human genome [6], which exerts influence on more than 60% of human protein-coding genes [7,8]. Therefore, miRNAs are considered to take part in almost all biological processes, such as cell apoptosis, differentiation, and proliferation [9]. MiRNA dysregulation has been involved in various disorders. In different kinds of cancers, different miRNA profiles have been revealed [10–12]. So far, more than 500 variants in miRNA genes have been identified [13]. Accumulating evidence demonstrates that mutation in miRNA genes or single nucleotide polymorphisms (SNPs) may affect target-binding activity, expression, or process of mature miRNA, thus affecting their target genes' expression [14,15]. As bunches of target genes may be regulated by a typical miRNA, functional SNPs in miRNA genes may exert influence on expression of numerous genes and consequently manipulate several signaling pathways, which may affect treatment response, prognosis, and susceptibility of human disease [16,17].

It has been shown that VEGF expression level is associated with the update of $^{18}$FDG [18], and we found VEGF is a virtual target of miR-125a by searching online the miRNA database (*www.mirdb.org*). One polymorphism (rs12976445) has been reported to be able to undermine the processing of the mature miR-125a and decrease the expression level of miRNA [19]. This association study is to explore the relationship between rs12976445 and uptake of $^{18}$FDG.

## Material and Methods

### Patients

The study comprised 169 individuals with primary non-small cell lung cancer (NSCLC) who were enrolled in our hospital from September 2013 to December 2014. Inclusion criteria for genotyping analysis were surgical candidate, diagnosed with primary NSCLC, with no history of primary chemotherapy treatment. From each participant 5 mL was obtained, and lung cancer tissue samples were available in 29 NSCLC patients. Written informed consent was obtained from each patients before the study. The study protocol was approved by the Ethical Committee (EC) and performed according to the Helsinki declaration of The Affiliated Hospital of Henan University of Science and Technology.

### FDG PET-computed tomography

All participants received a PET-CT scan before surgical intervention. Following 12 hours' fasting, $^{18}$FDG (3.7 MBq/kg) was given intravenously. Residual radioactivity and actual injected amount were determined using dose measurement system 50 min after radiotracer injection. PET-CT scans were conducted with a Discovery STE scanner (General Electric Medical Systems). A 3-dimensional ordered subset expectation maximization algorithm was used to reconstruct PET images.

### Quantitative PET measurements

The metabolic volume was defined as the 60% isocontour of the maximum pixel intensity automatically drawn on the lesion, and the radioactivity concentration was defined as the average radioactivity concentration within the metabolic volume. The background radioactivity concentration was obtained as the mean value of 4 circular ROIs positioned over the background around the lesion. The maximum standardized uptake value ($SUV_{max}$), defined as the uptake index least affected by partial volume effect, and the mean SUV ($SUV_{pvc}$) were measured using PVC method based on recovery coefficient (RC) curves, with all parameters normalized to weight.

### Genotyping

Salt precipitation method was applied to extract genomic DNA from peripheral blood samples. Single nucleotide extension was performed using a SNaPshot Multiplex System (Thermo Fisher Scientific). The chromosome segment covering the SNP was first

This work is licensed under Creative Common Attribution-NonCommercial-NoDerivatives 4.0 International (CC BY-NC-ND 4.0)



Indexed in: [Current Contents/Clinical Medicine] [SCI Expanded] [ISI Alerting System] [ISI Journals Master List] [Index Medicus/MEDLINE] [EMBASE/Excerpta Medica] [Chemical Abstracts/CAS] [Index Copernicus]

amplified through polymerase chain reaction (PCR). Primers and unincorporated deoxynucleotides (dNTPs)of the PCR products were removed by SAP and ExoI. Finally, dideoxyucleotide (ddNTP) extension (SNaPshot, Applied Biosystems) and fragment analysis were performed. Results were analyzed using the Peak scanner version 1.0 (Applied Biosystems). 5% of samples were selected randomly as replicates for quality control; reproducibility was 100%.

### Cell culture and oligonucleotide transfection

A549 cells were maintained in Dulbecco's Modified Eagle Medium/Nutrient Mixture F-12 (DMEM/F12) (HyClone, Logan, UT, USA) supplemented with 10% fetal bovine serum (Gibco, Grand Island, NY, USA) at 37°C in 5% $CO_2$ atmosphere. When the cells reached 80% to 90% confluence, the mimics/negative control, inhibitor/negative control of miR-125, and BIM small interfering RNA (siRNA) duplex oligonucleotides were transfected into A549 cells using riboFECT™ CP (RiboBio, Guangzhou, China), according to the manufacturer's protocol.

### RNA isolation

The mirVana™ miRNA Isolation Kit (Ambion) was applied to extract total RNA from the spinal cord tissues or A549 cells, in accordance with the manufacturer's instructions. After RNA was purified, a Nanodrop ND-1000 spectrophotometer (Infinigen Biotechnology) was used to determine the concentration of RNA.

### Quantitative real-time PCR detection of MiRNA expression

cDNAs were synthesized using TaqMan MicroRNA Reverse Transcription Kit (Applied Biosystems, Foster City, CA, USA). The PCR amplification for the quantification of the miR-125 and gene1 mRNA was performed with TaqMan miRNA Reverse Transcription Kit (Applied Biosystems) and TaqMan Human MiRNA Assay Kit (Applied Biosystems) on a 7500 real-time PCR system (Applied Biosystems). The comparative $2^{-\Delta\Delta}$Ct method was applied to calculate the relative expression of each miRNA, and results were normalized to snoRNA202.

### Luciferase reporter assay

Full-length 3-prime untranslated region (3' UTR) of the gene1 containing the 2 miR-125a-binding sites was amplified through PCR. The PCR primers used were as follows: forward primer 5'-GCGGTTCTCTTGTGGAGGGG-3'; reverse primer 5'-AGAAGGGGAAACGGCAGACA-3' and inserted into the restrictive sites of psi-CHECK™-2 vector (Promega, Madison, WI, USA). For mutant construct of gene1 3' UTR, site-directed mutagenesis was performed to generate the mutations. All constructs were confirmed by direct sequencing. A549 cells were cotransfected with the vectors (100 nM) containing wild-type or mutant 3' UTR and miR-124 mimics (100 nM) or control (100 nM; RiboBio) using riboFECT™ CP transfection kit, following the manufacturer's instructions. Forty-eight hours after transfection, luciferase assays were performed with a Dual-Luciferase Reporter Assay System (Promega), and the firefly luciferase activity was normalized to Renilla luciferase activity. Each experiment was performed 3 times.

### Western blotting

A549 cells or tissue samples were lysed with cell lysis buffer (Sigma-Aldrich, St Louis, MO, USA). After protein levels were measured, the lysates were loaded onto 10% polyacrylamide gel electrophoresis (PAGE) gel. The isolated protein was then transferred onto PVDF membrane. To avoid unspecific binding, the membranes were blocked with 5% nonfat milk solution. The blots were then incubated with the anti-VEGF (1:1000, room temperature) and anti-β-actin primary antibodies (1:10,000, room temperature) for 2 h. After being washed 3 times with TBST buffer, the blots were incubated with secondary antibody (1:10,000, room temperature) for another 2 h. Finally, the membranes were scanned and visualized using the Odyssey CLx imaging system (model number Ody-3086, LI-COR Inc, Lincoln, NE, USA). The primary anti-VEGF antibody and the anti-β-actin antibodies and secondary antibody (Cell Signaling Technology, Danvers, MA, USA) were chosen. The signals on the blots were detected using ECL kit (Pierce), and relative density of the target bands was determined normalized to β-actin, an internal control.

### Statistical analysis

Differences in selected variables and Hardy-Weinberg equilibrium were evaluated using the chi-square test and *t* test. Differences in the distributions of demographic characteristics and frequencies of genotypes between patients and control subjects were evaluated using *t* test (for continuous variables) or Pearson's chi-square test (for categorical variables). The odds ratios and 95% CIs were calculated by univariate and multivariate logistic regression analyses to determine associations. Adjusted odds ratios were computed using unconditional logistic regression with adjustment for age, sex, smoking, and drinking. $P<0.05$ was considered statistically significant. These statistical analyses were performed with the SPSS Software, version 12.0 (SPSS, Chicago, IL, USA), and were based on 2-tailed probability.

## Results

MiR-125a has been involved in many diseases, such as hepatocellular carcinoma and inflammation. In order to understand the role of MiR-125a in PET, we used online miRNA target prediction tools to search the regulatory gene of *miR-125a* and consequently identified VEGF as the candidate target gene of

This work is licensed under Creative Common Attribution-NonCommercial-NoDerivatives 4.0 International (CC BY-NC-ND 4.0)



Indexed in: [Current Contents/Clinical Medicine] [SCI Expanded] [ISI Alerting System] [ISI Journals Master List] [Index Medicus/MEDLINE] [EMBASE/Excerpta Medica] [Chemical Abstracts/CAS] [Index Copernicus]

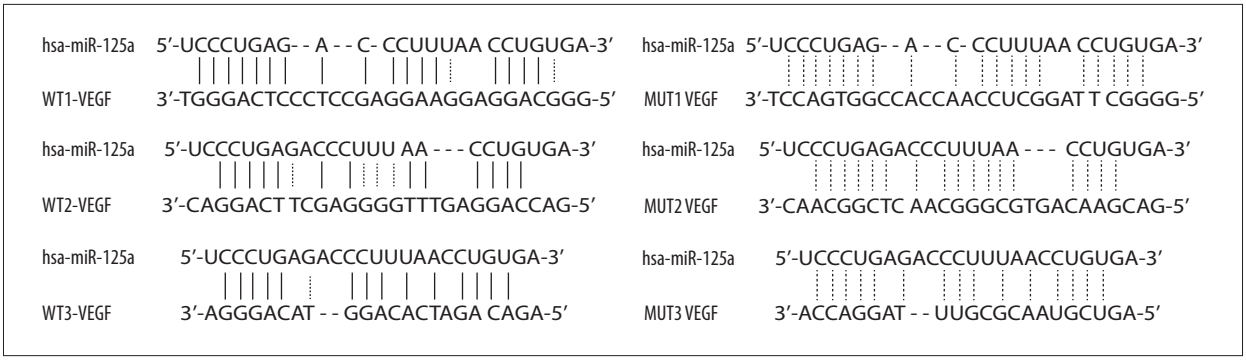


**Figure 1.** Vascular endothelial growth factor (VEGF) was the candidate target gene of miR-125a in A549 cells with the "seed sequence" in the 3-prime untranslated region (3' UTR); there were 3 binding sites.

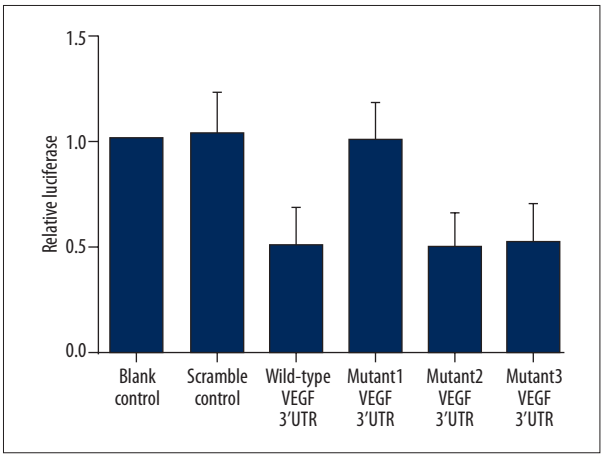


**Figure 2.** Luciferase activity reporter assay was conducted to verify vascular endothelial growth factor (VEGF) as the direct target gene of miR-125a.

*miR-125a* in A549 cells with the "seed sequence" in the 3' UTR (Figure 1) and there were 3 binding sites. Furthermore, to validate the regulatory relationship between miR-125a and VEGF, we also conducted luciferase activity reporter assay in A549 cells. We can see only the luciferase activity from the cells cotransfected with miR-125a and wild-type mutant2 and mutant3 VEGF 3' UTR: 3'UTR decreased significantly (Figure 2). Cells cotransfected with miR-125a and mutant1 VEGF 3' UTR were comparable to scramble control cells (Figure 2). The results confirmed that VEGF was a validated target of miR-125a in A549 cells.

### Determination of expression patterns of miR-125a and VEGF in tissues with different genotypes

The lung cancer tissue samples of 3 different genotypes (CC [n=18], CT [n=8], TT [n=3]) were used to further explore the impacts on the interaction between miR-125a and VEGF 3' UTR. Using real-time PCR, we found the expression of miR-125a increased in the GG group (Figure 3A) compared with the TT and CT groups; whereas the expression of VEGF mRNA (Figure 3B) was decreased in the CC group compared with the TT and CT groups. The expression of VEGF protein (Figure 3C) was measured by densitometry analysis, and we found it decreased in the CC group compared with the CT and TT groups.

To further validate the hypothesis of the negative regulatory relationship between miR-125a and VEGF, we investigated the mRNA/protein expression level of VEGF of A549 cells. We transfected the A549 cells with scramble control, miR-125a mimics, VEGF siRNA, and miR-125a inhibitors. As shown in Figure 4, the VEGF protein (Figure 4A) and mRNA (Figure 4B) expression levels of A549 cells treated with miR-125a mimics and VEGF siRNA were apparently lower than the scramble control, while cells treated with miR-125a inhibitors were apparently higher than the scramble control, validating the negative regulatory relationship between miR-125a and VEGF.

### Demographic, clinicopathologic, and genotypic parameters of the participants recruited in this study

We divided the participants into 3 groups by rs12976445 genotype. The CC group had 108 participants, and the CT+TT group had 61 (58+3). For the CC group, 64 participants were male and 44 were female. For the CT+TT group, 41 participants were male and 20 were female. The average age of the CC group was 59.34 y (SD, 12.1 y) and the average age of the CT+TT group was 59.82 y (SD, 11.8 y). The clinical grading in the CC group was 73 in G1/G2 and 35 in G3/G4. In the CT+TT group, 34 were G1/G2 and 27 were G3/G4. In the CC group, 62 were T0, 27 were T1/T2, 19 were T3/T4. For the CT+TT group, 37 were T0, 16 were T1/T2, 8 were T3/T4. In the CC group, participants with metastases were 24 and metastases-free participants were 84. For the CT+TT group, metastases participants were 16 and metastases-free participants were 45. The average SUVmax in the CC group was 9.23±3.45, whereas the average SUVmax in the CT+TT group was 8.92±3.24. The average SUVpvc of the CC group was 6.93±3.12, whereas the average SUVpvc of the CT+TT group was 6.47±3.21. The chi-square test was performed to evaluate the differences between CC and CT+TT groups among sex, age, grading, pT category, metastases, and FDG metabolism; all variables were statistically significant (Table 1).

This work is licensed under Creative Common Attribution-NonCommercial-NoDerivatives 4.0 International (CC BY-NC-ND 4.0)



Indexed in: [Current Contents/Clinical Medicine] [SCI Expanded] [ISI Alerting System] [ISI Journals Master List] [Index Medicus/MEDLINE] [EMBASE/Excerpta Medica] [Chemical Abstracts/CAS] [Index Copernicus]

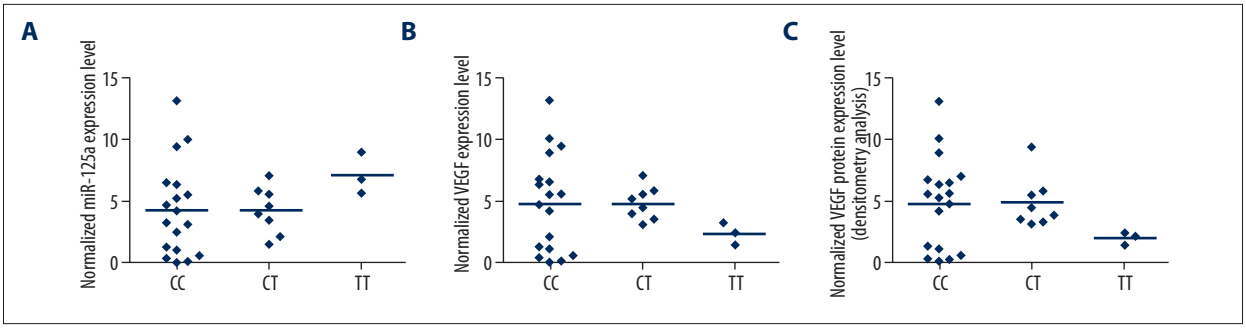


**Figure 3.** The expression of miR-125a increased in the GG group (**A**) compared with CT and TT groups while the expression of vascular endothelial growth factor (VEGF) mRNA (**B**) and protein (**C**) decreased in the CC group compared with CT and TT groups.

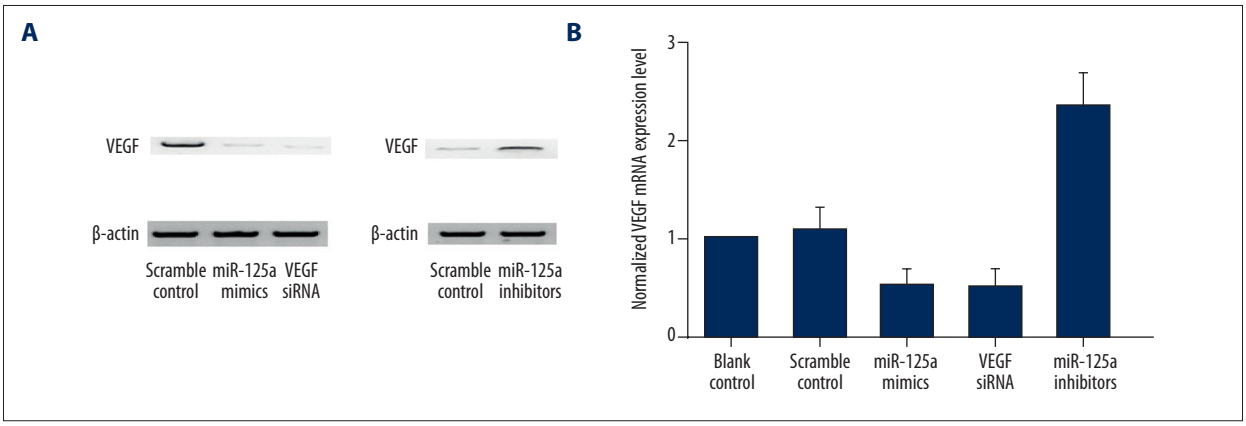


**Figure 4.** When transfected with the A549 cells with scramble control, miR-125a mimics, vascular endothelial growth factor (VEGF) small interfering RNA (siRNA), and miR-125a inhibitors, the expression level of VEGF protein (**A**) and messenger RNA (**B**) treated with miR-125a mimics and VEGF siRNA decreased, whereas cells treated with miR-125a inhibitors increased.

## Discussion

In this study, we used online miRNA target prediction tools to search the regulatory gene of miR-125a and consequently identified VEGF as the candidate target gene of miR-125a. We also conducted luciferase activity reporter assay in A549 cells; we can see only the luciferase activity from the cells co-transfected with miR-125a and wild-type VEGF 3' UTR and mutant2 and mutant3: 3' UTR decreased significantly (Figure 2). Cells cotransfected with miR-125a and mutant1 VEGF 3' UTR were comparable to scramble control cells (Figure 2). The results confirmed that VEGF was a validated target of miR-125a in A549 cells. Furthermore, the VEGF protein and mRNA expression level of A549 cells treated with miR-125a mimics and VEGF siRNA were apparently lower than the scramble control, whereas cells treated with miR-125a inhibitors were apparently higher than the scramble control, further validating the negative regulatory relationship between miR-125a and VEGF.

We discovered a remarkable association between [18]FDG uptake measured by PET and the miR-125a rs12976445 polymorphism in the current studies. The rs12976445 that corresponds to lower levels of VEGF is associated with lower [18]FDG uptake. This result is biologically plausible: VEGF serves as important regulator of permeability, vascular integrity, and angiogenesis [3]. A lower VEGF level-associated genetic variant, resulting to lower vascular density and growth, might possibly lead to lower [18]FDG uptake. In 2001, Bos et al. analyzed the relationship between [18]FDG uptake and various biomarkers [2]. In their research, plasma levels of VEGF did not show correlation with [18]FDG uptake. The tumor itself and several medications strongly influenced VEGF levels. Consequently, VEGF level measurements represent only "snapshots," and a high degree of variability might exist, which could obscure the exact relationship between certain phenotypes and biomarkers, such as VEGF.

Currently, few studies looked into the relationship between SNPs in miRNA and [18]FDG uptake, leaving this field poorly clarified and explored [18,20–24]. Our study examines the likely relationship between FDG-PET uptake and polymorphisms in miR-125a. As far as we know, our current research is the first work that assesses collective influence of the listed SNPs in miRNA on PET tracer uptake in NSCLC patients. [18]FDG uptake, expressed in terms of SUVpvc or SUVmax, depends largely on metabolism, and high values often correlate with reduced

This work is licensed under Creative Common Attribution-NonCommercial-NoDerivatives 4.0 International (CC BY-NC-ND 4.0)



Indexed in: [Current Contents/Clinical Medicine] [SCI Expanded] [ISI Alerting System] [ISI Journals Master List] [Index Medicus/MEDLINE] [EMBASE/Excerpta Medica] [Chemical Abstracts/CAS] [Index Copernicus]

**Table 1.** Demographic, clinicopathological and genotypic parameters of the participants recruited in this study.

| Rs2976445 genotype | CC | CT+TT | P value |
|---|---|---|---|
| N | 108 | 61 (58+3) | 0.709 |
| Sex | | | 0.803 |
| Male | 64 | 41 | |
| Female | 44 | 20 | |
| Age (years) | | | 0.126 |
| Mean | 59.34 | 59.82 | |
| SD | 12.1 | 11.8 | |
| Grading | | | |
| G1/G2 | 73 | 34 | |
| G3/G4 | 35 | 27 | |
| pT category | | | 0.747 |
| T0 | 62 | 37 | |
| T1/T2 | 27 | 16 | |
| T3/T4 | 19 | 8 | |
| Metastases | | | 0.556 |
| M (+) | 24 | 16 | |
| M (–) | 84 | 45 | |
| FDG metabolism | | | |
| SUV max | 9.23±3.45 | 12.92±4.24 | P<0.001 |
| SUV pvc | 6.93±3.12 | 8.47±3.21 | 0.002 |

overall survival of cancer patients [25]. Wolf et al. suggested that polymorphism that alter the expression level of VEGF, played a potential role on the variability of [18]FDG uptake in tumor tissue [18]. But the data reported by Lorenzen and our research findings do not verify this association [23].

In our study, we divided the participants into 3 groups by Rs2976445 genotype. The CC group had 108 participants, and the CT+TT group had 61 (58+3). The average SUVmax in the CC group was 9.23±3.45, whereas the average SUVmax in the CT+TT group was 8.92±3.24. The average SUVpvc of the CC group was 6.93±3.12, whereas the average SUVpvc of the CT+TT group was 6.47±3.21. The chi-square test was performed to evaluate the differences between CC and CT+TT groups for sex, age, grading, pT category, metastases, and FDG metabolism; all variables were statistically significant.

Rs2976445 has been reported to play a role in carcinogenesis of breast cancer [26]. miR-125a serves as a tumor suppressor in these malignancies. *In vitro* experiments indicated that the process of pre-miR-125a developing to its mature form might be affected by rs12976445 in pre-miR-125a [27]. Rs12976445 has been reported to be associated with cancer risk, and a C>T polymorphism in pri-miR-125a has been reported to be able to compromise the processing of the mature miRNA and reduce the expression level of the miRNA [19].

In this study, we discovered that rs12976445 TT genotype was implicated with a lower uptake rate of FDG. In this study, we collected lung cancer tissue samples of 3 different genotypes (CC=18, CT=8, TT=3) and found the expression of miR-125a increased in the CC group (Figure 3A) compared with the CT and TT groups, while the expression of VEGF mRNA (Figure 3B) decreased in the CC group compared with the CT and TT groups. The expression of VEGF protein (Figure 3C) was measured by densitometry analysis, and we found it decreased in the CC group compared with the CT and TT groups.

## Conclusions

Our study concludes that common rs12976445 polymorphisms have a significant impact on [18]FDG uptake in patients with NSCLC. Further study is needed to continue to promote the use of PET as a diagnostic tool.

### Conflict of interest

None.

This work is licensed under Creative Common Attribution-NonCommercial-NoDerivatives 4.0 International (CC BY-NC-ND 4.0)



Indexed in: [Current Contents/Clinical Medicine] [SCI Expanded] [ISI Alerting System] [ISI Journals Master List] [Index Medicus/MEDLINE] [EMBASE/Excerpta Medica] [Chemical Abstracts/CAS] [Index Copernicus]

## References:

1. Lee R, Yeung AW, Hong SE et al: Principles of medical oncology. Asian Pac J Surg Oncol, 2015; 1(1): 39–46
2. Bos R, Zhong H, Hanrahan CF et al: Levels of hypoxia-inducible factor-1 alpha during breast carcinogenesis. J Natl Cancer Inst, 2001; 93(4): 309–14
3. Carmeliet P, Jain RK: Angiogenesis in cancer and other diseases. Nature, 2000; 407(6801): 249–57
4. He L, Hannon GJ: MicroRNAs: Small RNAs with a big role in gene regulation. Nat Rev Genet, 2004; 5(7): 522–31
5. Bartel DP: MicroRNAs: Genomics, biogenesis, mechanism, and function. Cell, 2004; 116(2): 281–97
6. Macfarlane LA, Murphy PR: MicroRNA: Biogenesis, function and role in cancer. Curr Genomics, 2010; 11(7): 537–61
7. Friedman RC, Farh KK, Burge CB, Bartel DP: Most mammalian mRNAs are conserved targets of microRNAs. Genome Res, 2009; 19(1): 92–105
8. Mack GS: MicroRNA gets down to business. Nat Biotechnol, 2007; 25(6): 631–38
9. Krol J, Loedige I, Filipowicz W: The widespread regulation of microRNA biogenesis, function and decay. Nat Rev Genet, 2010; 11(9): 597–610
10. Kozinn SI, Harty NJ, Delong JM et al: MicroRNA profile to predict gemcitabine resistance in bladder carcinoma cell lines. Genes Cancer, 2013; 4(1–2): 61–69
11. Zhang C, Wang C, Chen X et al: Expression profile of microRNAs in serum: A fingerprint for esophageal squamous cell carcinoma. Clin Chem, 2010; 56(12): 1871–79
12. Yang Y, Li H, Hou S et al: The noncoding RNA expression profile and the effect of lncRNA AK126698 on cisplatin resistance in non-small-cell lung cancer cell. PLoS One, 2013; 8(5): e65309
13. Carbonell J, Alloza E, Arce P et al: A map of human microRNA variation uncovers unexpectedly high levels of variability. Genome Med, 2012; 4(8): 62
14. Hu Z, Chen J, Tian T et al: Genetic variants of miRNA sequences and non-small cell lung cancer survival. J Clin Invest, 2008; 118(7): 2600–8
15. Ling H, Spizzo R, Atlasi Y et al: CCAT2, a novel noncoding RNA mapping to 8q24, underlies metastatic progression and chromosomal instability in colon cancer. Genome Res, 2013; 23(9): 1446–61
16. Tian T, Shu Y, Chen J et al: A functional genetic variant in microRNA-196a2 is associated with increased susceptibility of lung cancer in Chinese. Cancer Epidemiol Biomarkers Prev, 2009; 18(4): 1183–87
17. Zhan X, Wu W, Han B et al: Hsa-miR-196a2 functional SNP is associated with severe toxicity after platinum-based chemotherapy of advanced non-small cell lung cancer patients in a Chinese population. J Clin Lab Anal, 2012; 26(6): 441–46
18. Wolf G, Aigner RM, Schaffler G et al: The 936C>T polymorphism of the gene for vascular endothelial growth factor is associated with $^{18}$F-fluorodeoxyglucose uptake. Breast Cancer Res Treat, 2004; 88(3): 205–8
19. Jiao L, Zhang J, Dong Y et al: Association between miR-125a rs12976445 and survival in breast cancer patients. Am J Transl Res, 2014; 6(6): 869–75
20. Grabellus F, Sheu SY, Bachmann HS et al: The XbaI G>T polymorphism of the glucose transporter 1 gene modulates 18F-FDG uptake and tumor aggressiveness in breast cancer. J Nucl Med, 2010; 51(8): 1191–97
21. Kim SJ, Hwang SH, Kim IJ et al: The association of 18F-deoxyglucose (FDG) uptake of PET with polymorphisms in the glucose transporter gene (SLC2A1) and hypoxia-related genes (HIF1A, VEGFA, APEX1) in non-small cell lung cancer. SLC2A1 polymorphisms and FDG-PET in NSCLC patients. J Exp Clin Cancer Res, 2010; 29: 69
22. Vänttinen M, Nuutila P, Kuulasmaa T et al: Single nucleotide polymorphisms in the peroxisome proliferator-activated receptor delta gene are associated with skeletal muscle glucose uptake. Diabetes, 2005; 54(12): 3587–91
23. Lorenzen S, Panzram B, Keller G et al: Association of the VEGF 936C>T polymorphism with FDG uptake, clinical, histopathological, and metabolic response in patients with adenocarcinomas of the esophagogastric junction. Mol Imaging Biol, 2011; 13(1): 178–86
24. Kalin NH, Shelton SE, Fox AS et al: The serotonin transporter genotype is associated with intermediate brain phenotypes that depend on the context of eliciting stressor. Mol Psychiatry, 2008; 13(11): 1021–27
25. Aldea M, Worni M, Dedivitis RA: Medical comorbidities in surgical oncology. Asian Pac J Surg Oncol, 2016; 2(3): 163–72
26. Li W, Duan R, Kooy F et al: Germline mutation of microRNA-125a is associated with breast cancer. J Med Genet, 2009; 46(5): 358–60
27. Hu Y, Liu CM, Qi L et al: Two common SNPs in pri-miR-125a alter the mature miRNA expression and associate with recurrent pregnancy loss in a Han-Chinese population. RNA Biol, 2011; 8(5): 861–72

This work is licensed under Creative Common Attribution-NonCommercial-NoDerivatives 4.0 International (CC BY-NC-ND 4.0)



Indexed in: [Current Contents/Clinical Medicine] [SCI Expanded] [ISI Alerting System] [ISI Journals Master List] [Index Medicus/MEDLINE] [EMBASE/Excerpta Medica] [Chemical Abstracts/CAS] [Index Copernicus]